Lidar studies of the cloud top in Western Siberia

I.E. Penner, G.P. Kokhanenko, and V.S. Shamanaev

Institute of Atmospheric Optics,
Siberian Branch of the Russian Academy of Sciences, Tomsk

Received December 3, 1999

Fluctuations of the cloud top (CT) were studied with an airborne lidar, and the spatial spectra of the CT were obtained. For the stratus they follow, on the whole, the "−5/3" power law. In some cases, the intensity of fluctuations of the atmospheric inhomogeneities with the scales less than 100 m decreases much faster. Horizontal dimensions of the CT inhomogeneities were found to obey the power-law distribution, while their vertical dimensions obey the exponential-law one. The empirical relation between the mean horizontal and vertical dimensions of the CT inhomogeneities was obtained.

Introduction

Many problems in atmospheric physics and climate strongly need for a more detailed knowledge of the statistical properties of the cloudiness. Comprehensive information on the spatial inhomogeneity of clouds can be obtained using lidars, which enable one to perform real-time and high-resolution study of the cloud geometry. Thus, for example, in 1993 two global experiments were conducted on sensing clouds over the land. These experiments involved 17 lidar groups from Europe, Asia, America, and Australia.[1] However, they mostly yielded data on the cloud base structure only, whereas the cloud top (CT) is the first the sunlight meets on its way to the land. Many researchers studying the radiative transfer in inhomogeneous clouds noted that it is very important to know the CT spatial structure. The most detailed review of the research in this field can be found in Ref. 2.

At the Institute of Atmospheric Optics, the CT was studied in 1986 (Ref. 3) with a Svetozar−3 lidar[4] mounted aboard an airborne laboratory. Experiments were conducted over land along the flight route up to 200 km as long. It was found that the rms fluctuations of the CT of low *St* clouds were 10−12 m. For *Sc* clouds with the mean CT at 2700 m and pronounced trends, fluctuations of the CT achieve 100 m even in single-layer clouds. For example, structures of the "turret" type of 200−250 m in diameter and 50−70 m in height, as well as those of the "minaret" type were analyzed. The height of the latter achieved 120−140 m at a diameter of 40 to 60 m. The first attempt to use spectral analysis in describing the CT height was also undertaken in this study,[4] although, without a detailed consideration of trends and low-frequency processes. At the same time, there is reason to believe that the statistical structure of land (continental) clouds differs from that of marine clouds, because the land surface is much more inhomogeneous than the sea surface on the scales of synoptic processes. This, in turn, must yield different heat fluxes and water vapor flows and, consequently, different cloud fields.

Preparation of the CT sensing data

In Ref. 5 we considered the results of two rather extensive experiments on sensing CT of stratus over the Arctic Ocean. For consistency with the results from Ref. 5, we used here the same threshold criterion for identifying the cloud boundary. The threshold was given by the signal from the atmosphere above the CT plus the doubled background noise present in the lidar return. In fact, it is the most sensitive criterion corresponding to the shortest distance from a lidar to a cloud boundary.[3] The CT height was calculated as a difference between the aircraft flight altitude determined from the data of the onboard navigation system and the distance to the CT determined using the onboard lidar system. We used the same procedures of preparing the initial arrays of data on CT prior to statistical analysis on the presence of high-frequency fluctuations. This is also true in case of revealing and eliminating linear trends and "jumps" in the CT height in the regions where different cloud fields are meet. For this purpose, a series of centered CT values $\{h_n\}$ was formed. Each data set was normalized by its rms deviation σ_h.

Thus, the experimental data acquired during individual flight days were reduced to the same scale. Besides, the mean height $\langle H_0 \rangle$ of clouds was determined for each measurement day in order to elucidate that the clouds under study belonged to the same family according to morphological cloud classification. Table 1 gives the general information on

0235-6880/00/04 348-07 $02.00

sensing the low-layer stratus in two flights over the Western Siberia.

Table 1. Initial data on sensing the CT over land with the airborne lidar used in the experiments

Characteristic	Western Siberia	
	June 25, 1994	Nov. 1, 1996
Type of clouds	*St–Sc*	*St*
Cloud amount	7–8	10
Height resolution, Δh, m	12	3
Spatial resolution along a flight, Δl, m	10	5
Mean height, H_0, m	1700	1600
Total length of sensing path, L, km	200	60
Number of CT values, N	16 000	12 000

Figure 1 shows two profiles of the CT height deviations relative to the zero mean for paths on different days. The CT fluctuations are given in units of the absolute standard deviation of the CT height σ_h for each experiment. Figure 1*a* shows the sensing data obtained with the laser pulse repetition frequency of 25 Hz (this means that about 12 000 measurements were conducted along a 60-km-long path). The profile shown in Fig. 1*b* was obtained as the laser operated at a pulse repetition frequency of 10 Hz; this corresponds to 12 280 measurements at a 120-km path. For such rather a long measurement series (L = 60 and 120 km), the difference in frequencies determining the spatial resolution along the path (Δl = 5 and 10 m, respectively) is already insignificant as concerning possible bias of the estimates of statistical moments of the first two orders.

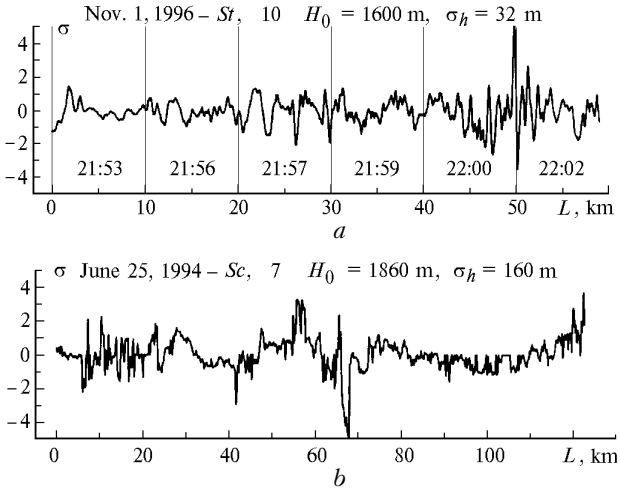

Fig. 1. Horizontal profiles of the relative CT height for paths of different lengths L. The value $\sigma = k\sigma_h$ is plotted as an ordinate; σ_h is the absolute rms deviation of the CT height for this experiment; H_0 is the mean CT height; fluctuations of the CT height are shown about the zero mean: *St*, cloud amount of 10 (*a*) and *Sc*, cloud amount of 7–8 (*b*).

The process of CT fluctuations in the newly formed series of relative heights $\{h_n\}$ can already be considered as approximately stationary as is seen from the shape of the distributions shown in Fig. 2. This figure shows the empirical histograms and their approximations by the Gaussian distribution for the data shown in Fig. 1. Each figure presents specific values of the single rms deviation σ_h obtained for the whole series $\{h_n\}$. As is seen, the fluctuations of the CT heights were higher (σ_h = 160 m) for the process studied on June 25, 1994, when multilayer broken cloudiness was observed. The continuous homogeneous field of stratus clouds observed on November 1, 1996, was characterized by lower fluctuation (σ_h = 32 m). The modal value of $p(h)$ for these cloud fields coincides with the position of the zero mean. The limiting σ_h deviation, except for extreme values of $\{h\}$, is within $\pm 3\sigma$. Although these realizations of the CT height were obtained in widely different cloud fields, the distribution of their statistical parameters has a similar characteristic shape, which is close to the normal one. Thus, standard methods of statistical analysis can be correctly applied to them.

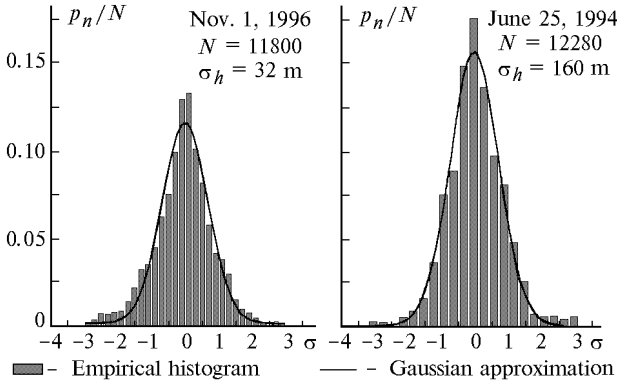

Fig. 2. Empirical histograms of centered fluctuations of the CT height for Figs. 1*a* and *b* and their Gaussian approximations.

Spatial spectrum of the stratus CT fluctuations

The spectral density of fluctuations of the CT height was estimated following the algorithms described earlier in Ref. 5 as a function $S_h(k_i)$ of spatial wave number $k_i = 2\pi/\lambda_i$ (see Ref. 6):

$$S_h(k_i) = \frac{2}{n_d\, N\, \Delta\lambda} \sum_{j=1}^{n_d} |\, H_j(k_i)\,|^2, \quad i = 0, 1, \ldots, N/2,$$

where $H_j(k_n)$ is the finite Fourier transform of the data sample $\{h_{jn}\}$ ($n = 0, 1, \ldots, N-1$; $j = 1, 2, \ldots, n_d$).

Thus, Fig. 3 shows the spectra $S_h(k)$ for a sample of individual measurements for the flight route

considered in Fig. 1*a*. These data samples were obtained with high spatial resolution $\Delta\lambda$ ($\Delta\lambda \approx 3.5$ m with the aircraft flight speed of 85–90 m/s). This allowed the spectral density to be estimated within 20% error at a sufficiently high frequency (for cloud formations) spectral region in the spatial wavelength band $7 < \lambda < 200$ m.

Spectral estimates in the spatial wavelength region $12 < \lambda < 120$ m are closely approximated by the power dependence $S_h(k) \sim k^{-p}$. The spectrum is restricted in the region of small wave numbers, because it rolls off due to elimination of low-frequency components, whose assumed period exceeds the duration of the analyzed realization $\{h\}$. This is especially well seen in the spectrum obtained from the data sample recorded at 21:53 (see Fig. 1*a*). In this case, elimination of the low-frequency trend from the sample $\{h_n\}$ significantly depleted the process of fluctuations at the wavelengths $\lambda > 100$ m. The restriction in the region of high-frequency fluctuations at the wavelengths about 10 m is explained by the markedly lower drop rate of the spectral density, what is more characteristic of "white noise" processes. It should be noted that even for such small-scale fluctuations of the CT height we did not reach the viscosity wavelength region, in which, according to the theory of atmospheric turbulence,[7] kinetic energy of turbulent motions transferred by cascade processes dissipates. This interval of spatial scales in cloud formation processes is characteristic of disintegration and degeneration of cloud structures.

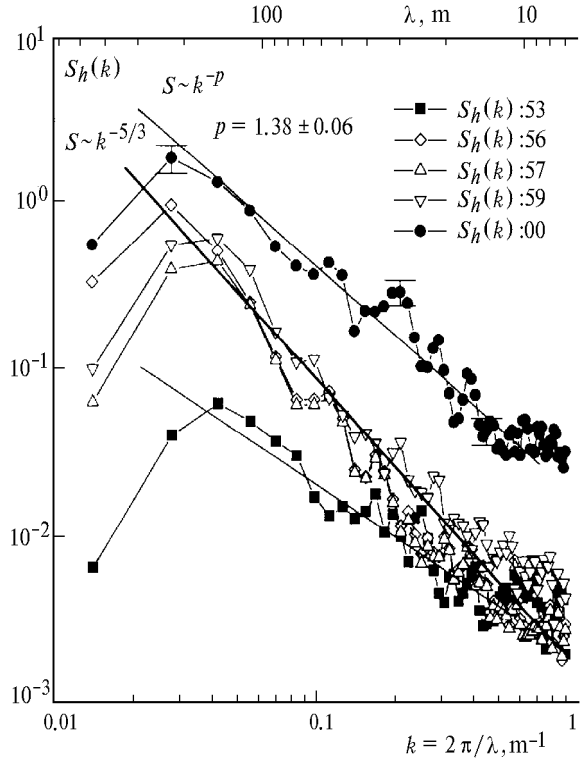

Fig. 3. Spatial spectra of the CT height fluctuations for some data samples presented in Fig. 1*a*. The time at which the data samples were acquired is shown nearby the curves.

For some spectral functions $S_h(k)$ the approximating straight lines (in the case of double logarithmic scale in Fig. 3) of the power dependence plotted in the region of spatial wavelengths under study give a markedly less slope. One of the reasons of such a behavior of the spectral density function obtained from the data recorded at 22:00 is an extra energy (relative to the energy of the averaged turbulent motion of the atmosphere in the inertial interval) from vertical motions of atmospheric formations due to ambient conditions (possibly, due to a nonuniform surface). This is demonstrated by the intensity of fluctuations on the scales with the spatial wavelengths from 20 to 60 m, which is pronounced in the spectral density (Fig. 3, $S_h(k)$ at 22:00).

Most of the spectra shown in Fig. 3 have the slope close to the "–5/3" law and differ insignificantly in the exponent p. This dependence keeps within the estimate of the spectrum calculated from the samples over the entire flight route (Fig. 1*a*). Figure 4*a* demonstrates that this regularity keeps in the entire region of the analyzed spatial wavelengths $0.007 < \lambda < 7$ km. Let us recall that here we consider a sufficiently homogeneous field of *St* clouds, for which the standard absolute deviation of the not centered CT height σ_1 equaled to 32 m.

Spatial spectrum of CT fluctuations in stratocumulus

The cloud field of another kind, whose horizontal height profile is shown in Fig. 1*b*, consists of stratocumulus (*Sc*) clouds with the cloud cover index of 7–8 and the broken multilayer structure with the rms deviation $\sigma_1 = 160$ m. In this connection, the attention should be paid to the fact that the considered CT profile was constructed using mostly the heights of the upper layer of the cloud system under study (of the same lower level). The upper layer was more dense, and no layer intermittence occurred.

The spectral density estimated from individual samples of data on the CT fluctuations along the flight route over this cloud field differs widely both in the spectral shape and in the characteristic slope of the spectrum. That is why Fig. 4*b* shows only smoothed spectrum $\bar{S}_h(k)$ averaged over all realizations in the spatial wavelength region $0.017 < \lambda < 4.4$ km. This spectral estimate accurate to the error no more than 15% provides the high reliability of the statistical stability and thus characterizes, in the general form, the dynamics of cloud fields in the spectral region analyzed.

As is seen from Fig. 4*b*, in the region of small wave numbers ($k < 0.04$ m^{-1}) the inertial interval of spatial scales is pronounced. The spectral density in this interval is approximated by the "–5/3" power law. Then, as k increases, the inflection of the spectrum is seen at the scales with $\lambda \approx 100$ m. The inflection is

followed by the faster, than in the inertial interval, drop of the spectral density in the region of large wave numbers. In the inflection zone, the drop of the spectral density of CT height fluctuations slows down. At these spatial scales, the turbulent energy receives an extra energy due to convective motions in cumulus. It follows from the fact that thermal turbulence elements generated by such motions inside a cloud have characteristic scales corresponding to the wave numbers in the inflection zone ($0.04 < k < 0.1$ m^{-1}) (Ref. 8).

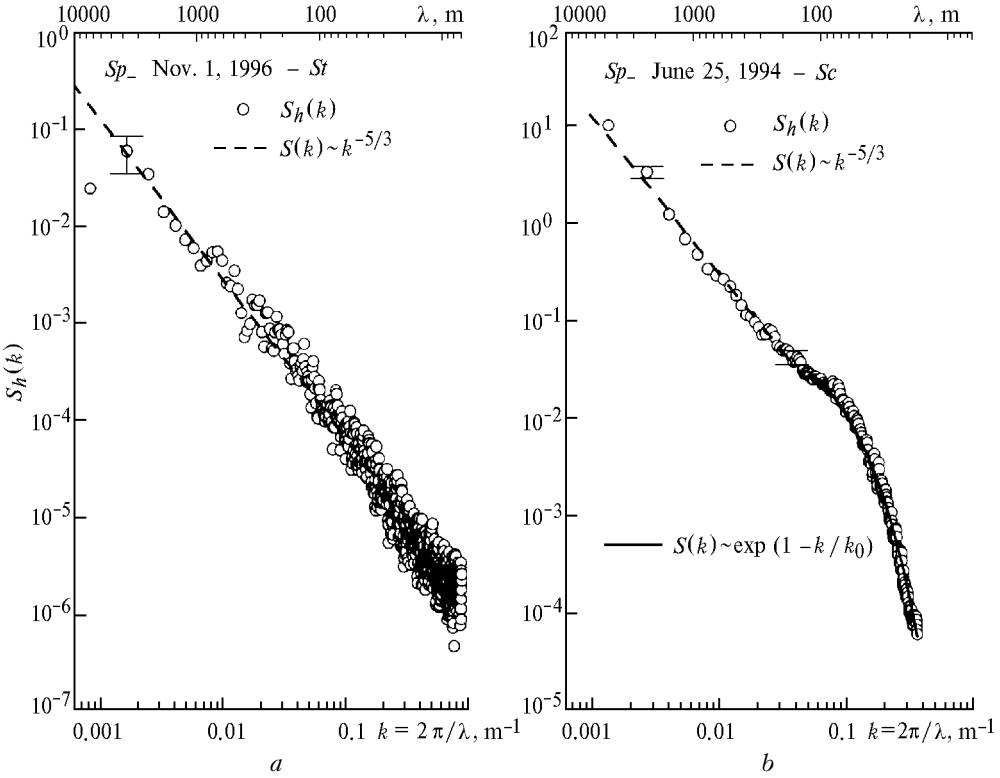

Fig. 4. Spatial spectra of the CT height fluctuations for flights shown in Fig. 1: Fig. 1*a*, *St*, cloud amount of 10 (*a*) and Fig. 1*b*, *Sc*, cloud amount of 7–8 (*b*). The dashed curve is for the Kolmogorov–Obukhov "–5/3" law; solid curve in Fig. 4*b* is for the approximation by the exponential distribution law.

In the region of large wave numbers ($k > 0.1$ m^{-1}) the spectral density curve drops down steeply. As the approximating region of wave numbers $0.1 - 0.2 < k < 0.36$ m^{-1} of this spectrum narrows toward the maximum value, the exponent of the power dependence increases from three to five in its absolute value. The regularity of the physical processes of CT height fluctuations in the spectral region with $k > 0.04$ m^{-1} differs clearly from the power dependence. In this region, the drop of the spectral density can be well approximated by the exponential dependence of the following form:

$$S(k) \sim \exp(1 - k/k_0), \quad k > k_0,$$

where k_0 is the wave number of the beginning of the inflection zone. Such an exponential dependence of the spectral density drop was proposed in the theoretical model of spectral transfer of the turbulent energy in the viscous spectral region. This model is based on the Heisenberg hypothesis assuming that the mechanism of energy transfer from large vortices to small ones is similar to the process of viscous dissipation, in which large vortices loss their energy for the work against friction forces initiated by smaller turbulent vortices.[9]

Thus, the spectral density of height fluctuations $S_h(k)$ decreases, after the inflection point at the spatial scales, at which the extra energy comes from convective turbulent motions inside *Sc* clouds, more steeply as compared with the inertial interval of wave numbers because of viscous degeneration of small-scale vortices of thermal turbulence on their way to the top of *Sc* clouds. The degeneration process can be intensified due to the energy loss of vertical motions of cloud convection elements arising (because of the Archimedean forces of positive buoyancy) against negative buoyancy in the stable inversion layer at the top of stratocumulus clouds. The effect of the physical process of degeneration is the stronger, the less are thermal turbulence elements and the more stable is the over-cloud inversion layer.

Note that for the whole set of our lidar measurements over land, the spectrum $S_h(k)$ of fluctuations of the stratocumulus top keeps the shape shown in Fig. 4*b*. The spectrum of CT fluctuations of

marine stratocumulus[5] also has an inflection although a less pronounced one.

Regularities in the distribution of horizontal dimensions of the CT inhomogeneities

The data of sensing the CT allowed us to reveal some statistical properties of the distribution of horizontal dimensions of the CT inhomogeneities. Figure 5 shows the scheme of fragmentation of the cloud top boundary into cloud segments in a vertical sensing cross sections. For each height level of the horizontal cross section, H_0, $H_0 + \sigma_h$, and $H_0 - \sigma_h$ (where H_0 is the level of the mean CT height, and σ_h is the standard deviation), segments with the corresponding length L_s and height H_s were separated out. The total number of the segments for the 220-km long flight path was 3217.

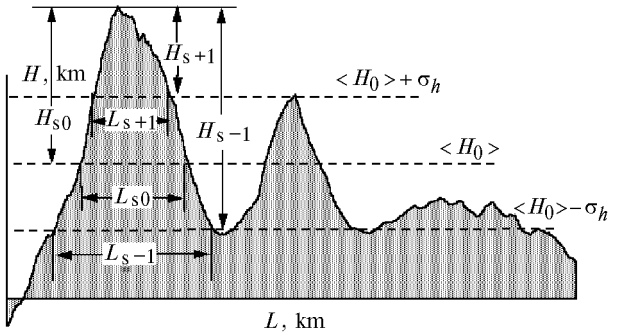

Fig. 5. Scheme of CT fragmentation into cloud segments at its cross sections in the vertical plane.

Figure 6 shows 1D distributions of the number of cloud segments vs. length L_s (Fig. 6*a*) and height H_s (Fig. 6*b*). The distributions were obtained for all the sensing paths at the level of the mean height H_0. It is seen that the regularities of the statistical distribution of the inhomogeneities in the vertical and horizontal planes have different character. The approximation of the H_s distribution by the exponential dependence corresponds to the normal (Gaussian) distribution law, which was determined from the empirical histogram (Fig. 2). At the same time, the distribution of horizontal dimensions L_s has pronounced power dependence. This is demonstrated by high correlation ($R = 0.98 \pm 0.13$) between the approximating straight line of the linear regression (on the double logarithmic scale) and experimentally measured points of the distribution. The parameter of the slope gives the exponent of the power dependence $p = 1.95 \pm 0.05$. The mean segment length is $\langle L_s \rangle \approx 110$ m, what agrees well with the scale of an inhomogeneity separated in the inflection zone of the spatial spectrum of the CT fluctuations (Fig. 4*b*). A similar power dependence of linear dimensions of the cloud inhomogeneities in the field of reflected radiation obtained from the satellite (LANDSAT) data has been published in Ref. 10.

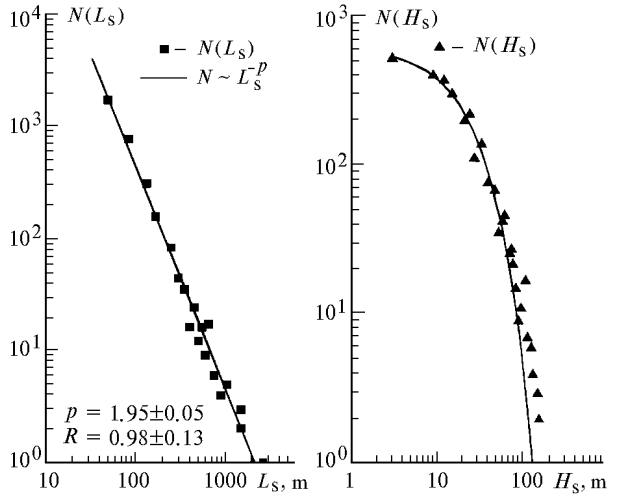

Fig. 6. One-dimension distributions of the number of cloud segments over their lengths L_s (*a*) and heights H_s (*b*).

An interesting effect was revealed when analyzing the probability density of L_s distributions (Fig. 7) obtained at different levels of horizontal cross section of an inhomogeneous cloud field (for example, Fig. 1*a* shows the vertical profile of *St* clouds). It is seen that the power law of the dependence of the size distribution works at all cross sections, but the exponent decreases (in the absolute value) as the height of the cross section decreases. Such a behavior of the 1D L_s distributions at different levels characterizes the property of the scale invariance of cloud spatial structures in the horizontal plane and anisotropy of the 2D field in the vertical direction. This behavior may be partially caused by insufficient statistics on segment dimensions at different levels in a limited cloud field (the total number of segments $N_{sum} = 585$). However, estimates of the spectral density of the CT fluctuations of this field ($S_h(k)$ in Fig. 4*a*) are indicative of the presence of fluctuations of all length scales and their homogeneous distribution over the whole inertial wavelength region.

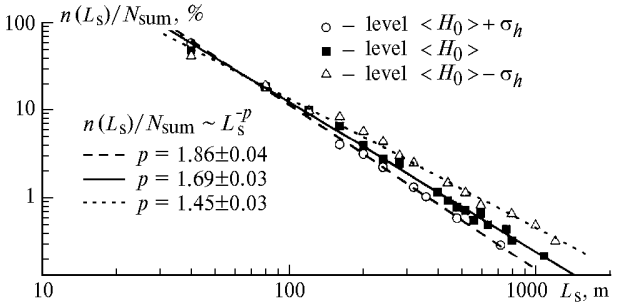

Fig. 7. Probability density of L_s distributions at different levels of horizontal cross sections as shown in Fig. 5.

Reference 11 described how the exponent of the power dependence of the distribution changes in response to the threshold criterion of determination of

the outer scale of the inhomogeneities in the fragmented layers of *cumulus* clouds. (The indicator function of cloud segments was constructed in Ref. 11 based on the threshold concentration of droplets with the diameter less than 30 μm measured at the same level of the horizontal cross section height.) The main tendency of this change is a decrease in the absolute value of the exponent with the increasing outer scale of the cloud segments. This coincides with the regularity we revealed in the change of statistics of fluctuations along the horizontal dimensions of the inhomogeneities, as the cross section levels are deeper into the *stratus* clouds.

The nonlinear dependence we have revealed in vertical and horizontal dimensions of cloud inhomogeneities is a very interesting result. This gives us quantitative data on anisotropy of the 3D structure of the CT height. Figure 8 shows the dependence of the dimensionless height $\langle H_s/\Delta h\rangle_{L_s}$ on the dimensionless length $L_s/\Delta l$ of a cloud segment on the double logarithmic scale. Here Δh and Δl denote respectively the steps of the spatial resolution in the vertical and horizontal directions, and the brackets are for the averaging of heights in segments having the same length L_s. The linear regression parameter B [from the equation $\log(H_s/\Delta h) = A + B \log(L_s/\Delta l)$] that determines the slope of the approximating straight line constructed using the empirical points in Fig. 8 corresponds to the scaling index α (Ref. 12) in the similarity relation of linear dimensions of the cloud segments:

$$H_s/\Delta h \approx (L_s/\Delta l)^{\alpha}.$$

Here the exponent α describes the degree of increase of the cloud segment height as its length increases. The value $B = 0.50 \pm 0.02$ found gives $\alpha \cong 1/2$, that is, the height of a cloud segment increases, on the average, as the square root of its length.

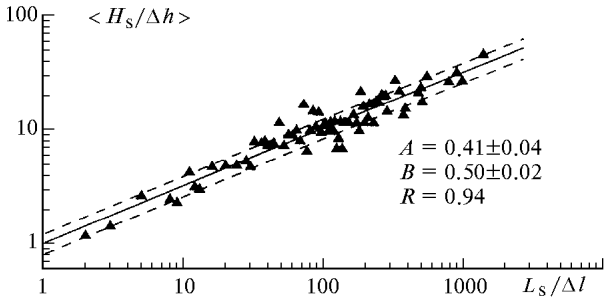

Fig. 8. Mean dimensionless height of inhomogeneities vs. dimensionless length of segments of cloud inhomogeneities.

Conclusion

The data of sensing the cloud top with an airborne lidar system upon being analyzed have allowed us to reveal some regularity in the distribution of spatial inhomogeneities. We have also estimated quantitatively the statistical parameters of the stochastic spatial structure of stratus and stratocumulus low-layer clouds.

The probability density of the distribution of the length of an inhomogeneity in the CT is a power function. The probability density of the distribution of the inhomogeneity height is an exponential function. According to our data, the height of the inhomogeneities in the top of stratus clouds increases, on the average, proportionally to the square root of their length.

The spatial spectra of fluctuations of the CT height of clouds of this morphological family correspond, on the whole, to the Kolmogorov–Obukhov power law. At long sensing ranges and for large-scale inhomogeneities in cloud fields of both kinds the exponent is close to "−5/3." However, for stratocumulus clouds or for stratus clouds being in the process of dissipation, starting from 200-m long and shorter inhomogeneities, the spectra of fluctuations decrease faster thus approaching the "− 13/3" law. The similar spatial spectrum of the reflected radiation with the characteristic break at the comparative scales in the field of the radiative temperature of stratocumulus clouds reconstructed from the satellite LANDSAT data was obtained in Ref. 10. Recently, the causes of such a "strange" behavior of the reflected radiation have been discussed in the literature quite intensively.[13–15]

Hypotheses directly based on smoothing of small-scale fluctuations of the radiative field due to the effects of the horizontal transfer of radiative fluxes were put forward,[14] as well as hypotheses based on inhomogeneity of the spatial structure of cloudiness and the influence, in this connection, of geometrical averaging[13] due to a finite field of view of actual receivers. Titov[15] critically analyzed drawbacks in explanation of the spectral break by radiative smoothing. He also studied in Ref. 15 the effect of geometrical averaging on the spatial spectrum of reflected radiation in inhomogeneous stratocumulus clouds by numerical simulation and concluded that this effect manifests itself clearly at a large field of view of a detector of reflected radiation and it should be taken into account when interpreting satellite data. However, at the same time, because of the high spatial resolution (about 30 m for LANDSAT data) and, consequently, very small detector's field of view, the geometric averaging effect likely fails to explain the break in the spatial spectra of the reflected radiation.[15] Titov assumed that the spectral break is likely the consequence of the spatial inhomogeneity of actual cloud fields.

In our opinion, the latter assumption is of primary importance among the possible causes resulting in the break of the spectral density of some spatially distributed characteristics in a stratocumulus cloud field. This is likely demonstrated by the spatial spectra of the CT height fluctuations presented in this paper and in Ref. 5 that characterize different statistical

structure of inhomogeneities at different spatial scales. If we take into account that the cloud top boundary plays the role of an indicator of cloud formation dynamics, we can conclude that the characteristic scale of the spectral break is a sort of a boundary between different physical processes determining the intensity of fluctuations of spatial cloud characteristics on the corresponding scales. One of the most probable scenarios of evolution of such a process resulting in smoothing of small-scale inhomogeneity fluctuations of stratocumulus clouds and, consequently, in the break of the spatial spectrum has been considered in this paper.

References

1. C.M. Platt, S.A. Young, A. Carswell, S. Pal, M.P. McCormick, D. Winker, F. DeGuasta, W. Eberhard, P. Flamant, B. Forgan, G. Gimmestad, M. Hardesty, S. Khmelevtsov, I. Kolev, Lu Darren, K. Sassen, V. Shamanaev, L. Stefanutti, O. Uchino, U. Wandinger, C. Weitkamp, C. Wooldridge, and H. Yager, Bull. Amer. Meteorol. Society **75**, No. 9, 1635–1654 (1994).
2. G.A. Titov and E.I. Kassianov, Atmos. Oceanic Opt. **12**, No. 10, 873–882 (1999).
3. I.E. Penner, I.V. Samokhvalov, V.S. Shamanaev, and I.A. Shnaider, in: *Procs. of the 9th All-Union Symp. on Laser and Acoustic Sensing on the Atmosphere* (Tomsk, 1987), Part 1, pp. 212–216.
4. V.E. Zuev, ed., *Laser Sensing of the Troposphere and Underlying Surface* (Nauka, Novosibirsk, 1987), 262 pp.
5. I.E. Penner and V.S. Shamanaev, Atmos. Oceanic Opt. **12**, No. 12, 1093–1097 (1999).
6. J.S. Bendat and A.G. Piersol, *Random Data: Analysis and Measurement Procedures* (Willey, New York, 1966).
7. V.I. Tatarskii, *Wave Propagation in a Turbulent Medium* (Dover, New York, 1968).
8. N.K. Vinnichenko, N.Z. Pinus, S.M. Shmeter, and G.N. Shur, *Turbulence in the Free Atmosphere* (Gidrometeoizdat, Leningrad, 1976), 288 pp.
9. D.L. Laikhtman, ed., *Dynamic Meteorology* (Gidrometeoizdat, Leningrad, 1976), 608 pp.
10. R.F. Cahalan and J.B. Snider, Remote Sens. Environ. **28**, 95–107 (1989).
11. C. Duroure and B. Guillemet, Atmospheric Research **25**, No. 4, 331–350 (1990).
12. B.B. Mandelbrot, *The Fractal Geometry of Nature* (W.H. Freeman, New York, 1983).
13. H.W. Barker, Remote Sens. Environ. **54**, 113–120 (1995).
14. A. Davis, A. Marshak, R. Cahalan, and W. Wiscombe, J. Atmos. Sci. **54**, No. 2, 241–260 (1997).
15. G.A. Titov, Atmos. Oceanic Opt. **12**, No. 3, 180–186 (1999).